J. Fluid Mech. (2003), *vol.* 483, *pp.* 91–109. © 2003 Cambridge University Press
DOI: 10.1017/S0022112003003951 Printed in the United Kingdom

Dipole solutions for viscous gravity currents: theory and experiments

By STUART E. KING AND ANDREW W. WOODS

BP Institute, University of Cambridge, Madingley Rise, Madingley Road, Cambridge, CB3 0EZ, UK

(Received 21 March 2002 and in revised form 29 August 2002)

We describe the gravity-driven flow of a viscous fluid in a semi-infinite porous layer, $x > 0$, from which fluid can drain freely at $x = 0$. New experiments using a Hele-Shaw cell confirm that when the base of the layer is impermeable the motion of the current is self-similar and the dipole moment of the flow is conserved, as proposed theoretically by Barenblatt & Zel'dovich (1957). We extend the model to allow fluid to drain through the base of the porous layer into a thin horizontal layer of lower permeability. In this case we predict that the dipole moment of the current decays exponentially with time. At early times we find that the loss of fluid from the gravity current in the high-permeability layer is dominated by the draining at $x = 0$, whereas at long times, the gravity-driven leakage into the underlying low-permeability layer is dominant. We successfully compare these analytic solutions for such draining currents with further laboratory experiments in which fluid drains from the end and through the base of a Hele-Shaw cell. We discuss the implications of these results for the dispersal of chemicals or pollutants injected into a layered porous rock.

1. Introduction

Gravity-driven flows in porous rocks arise in a number of engineering and natural situations in which fluid of one density invades a porous layer saturated with fluid of a different density. Important examples arise in hydrocarbon reservoirs in which chemical-laden water is injected to sweep oil or to dissolve precipitate and increase the permeability of the rock. If a finite volume of fluid is injected into the reservoir then, following the injection period, the flow spreads under the influence of gravity. In studying such flows, we are especially interested in the dispersal of fluid through the formation. Many reservoirs involve complex layering. In such situations fluids tend to spread laterally along high-permeability layers and then gradually drain into adjacent low-permeability layers (Pritchard, Woods & Hogg 2001; Pritchard & Hogg 2002). However once the flow is driven by gravity, some of the injected fluid may flow back and drain into the source well, thereby being lost from the system (figure 1). An analogous flow regime also develops with groundwater flow through fractured porous rocks: at periods of high water a fluid may invade the porous matrix from a fracture and subsequently spread through the formation; as the water level drops the fluid may be able to drain back into the source fracture as it continues to spread through the porous rock.

The geometry of such flows may be two-dimensional if fluid spreads from a near horizontal well or from a fracture into the neighbouring formation, whereas the flow may be axisymmetric if it spreads rapidly from a localized vertical well. Here we focus on the two-dimensional case, corresponding to injection from a horizontal well

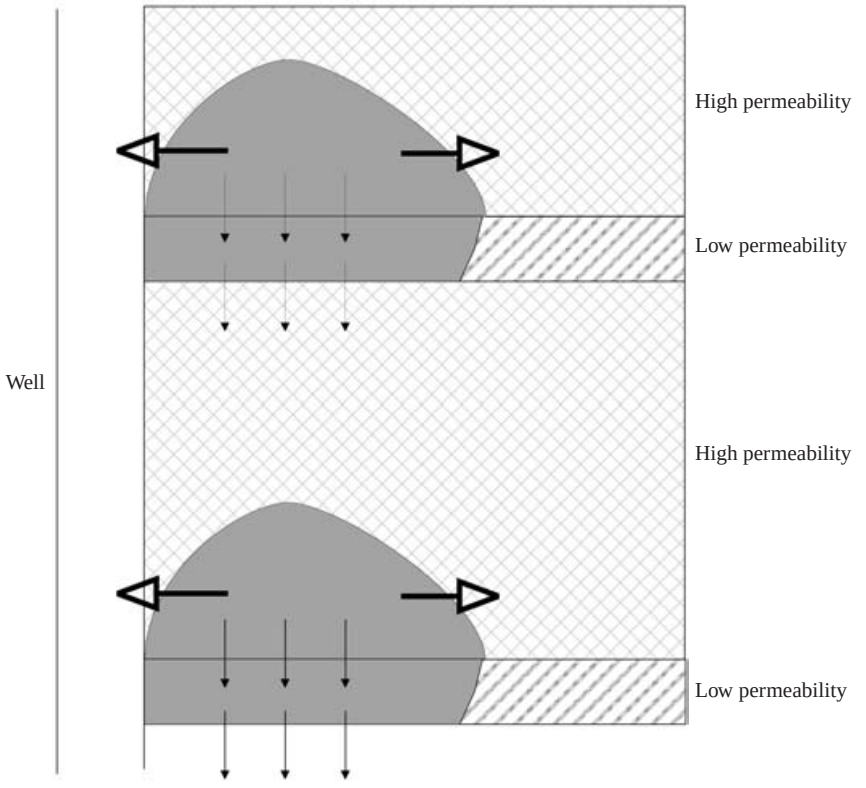

FIGURE 1. Diagram showing a fluid supplied to a stratified rock from a well; fluid moves along high-permeability layers, slowly draining into adjacent low-permeability layers and also draining back into the well bore.

or fracture. We neglect the effect of capillary forces, as is appropriate for miscible displacement or large-scale immiscible flows.

First we examine the case in which there is no draining within the formation. For the release of a finite volume of fluid, Barenblatt & Zel'dovich (1957) (see also the book Barenblatt, Entov & Ryzhik 1990) showed that as the fluid propagates into the medium $x > 0$ and drains at $x = 0$ then, if the current has free surface of height $h(x, t)$ and horizontal extent $L(t)$, the dipole moment Q, defined by

$$Q = \int_0^{L(t)} xh(x, t)\,\mathrm{d}x, \tag{1.1}$$

remains constant. This constraint leads to a class of similarity solution for such flows and we build on this work in the present paper. We present a series of new laboratory experiments which test relation (1.1), and the similarity solution of Barenblatt & Zel'dovich (1957). We then extend the model and experiments to include the effects of draining through the base of the layer. We examine the balance between the loss of fluid at the source $x = 0$, and the draining into the adjacent low-permeability structure. We develop some new analytic solutions and test these with new laboratory experiments. Our results show that the loss of fluid at the source region leads to a substantial difference in the intrusion distance of the current and in the amount of fluid transferred to the formation compared to the case where there is no draining at the

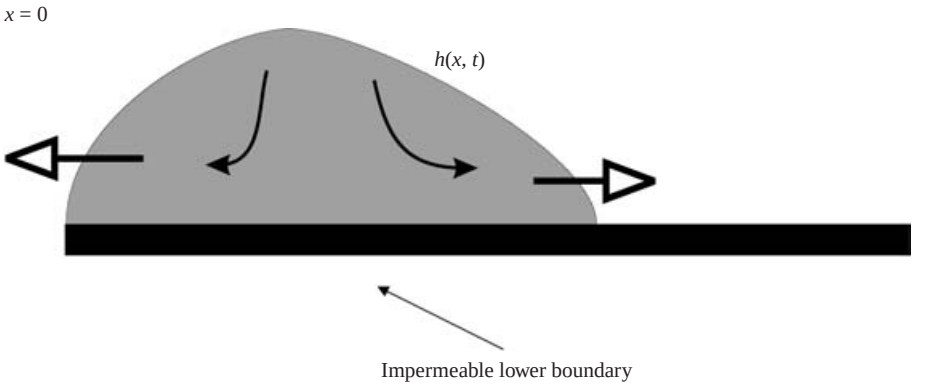

FIGURE 2. Diagram showing the spreading of a mound of fluid over an impermeable base through a medium of permeability K with free draining at $x = 0$.

source (Pritchard *et al.* 2001). We generalize this modelling approach to describe the motion of a two-dimensional free-surface viscous gravity current. Again we present some analytic solutions and verify these with laboratory experiments.

2. Dipole solution for a gravity current in a porous medium

2.1. *Theory*

The gravity-driven motion of a mound of viscous fluid which spreads along the horizontal impermeable base of a porous medium (see figure 2) under the assumption that it is relatively thin (pressure in the fluid is assumed to be hydrostatic) and that the Reynolds number of the flow is small, may be described by the equation

$$h_t = \Omega(hh_x)_x, \tag{2.1}$$

where $h = h(x, t)$ is the height of the free surface of the mound at a distance x from the origin and time t, and where

$$\Omega = \frac{K\Delta\rho g}{\mu}. \tag{2.2}$$

Here $\Delta\rho$ is the density difference between the current and the ambient fluid in the permeable rock, K is the permeability, and μ the viscosity of the fluid. This equation is well-studied in the context of porous media and is due to Boussinesq (1903). Derivations and applications of equation (2.1) can be found in the books by Bear (1972), Turcotte & Schubert (1982), Barenblatt *et al.* (1990), and others on groundwater flow.

We now examine the motion of a finite release of fluid in the region $x > 0$, subject to the constraint that the free-surface height $h = 0$ at $x = 0$ while the volume flux hh_x takes some finite value at $x = 0$. For this problem Barenblatt & Zel'dovich (1957) showed that the dipole moment Q defined by

$$Q = \int_0^{L(t)} xh(x, t)\,\mathrm{d}x, \tag{2.3}$$

is invariant, where $L(t)$ is the lateral extent of the current, and $h(L) = 0$. This can be shown by combining equation (2.1) with the additional assumption that h_x is

non-singular at $x = L$ as follows:

$$\frac{\mathrm{d}}{\mathrm{d}t}\int_0^L xh(x,t)\,\mathrm{d}x = L\dot{L}h(L,t) + [x(hh_x)]_0^L - \left[\tfrac{1}{2}h^2\right]_0^L = 0. \tag{2.4}$$

Since there are no external length scales associated with this flow the system admits self-similar solutions of the form

$$h = Bt^{\beta} f(\eta), \tag{2.5}$$

where $\eta = x/At^{\gamma}$ is the non-dimensional similarity variable, and A, B are constants to be found by dimensional analysis. By substitution into equation (2.1), and use of the constraint (2.3) the solution is found to be

$$\left.\begin{aligned} h(x,t) &= \left(\frac{Q}{\Omega}\right)^{1/2} t^{-1/2}\tfrac{1}{6}\left((40)^{3/8}\eta^{1/2} - \eta^2\right), \\ \eta(x,t) &= \frac{x}{(Q\Omega)^{1/4}t^{1/4}}, \end{aligned}\right\} \tag{2.6}$$

as was presented by Barenblatt & Zel'dovich (1957) in the context of the flooding and subsequent draining of a porous medium by groundwater. An alternative approach to this solution is discussed in appendix A.

2.2. *Experiments*

To test this theoretical model we conducted some new experiments in a Hele-Shaw cell. This is an analogue for flow in a fracture and also for two-dimensional flow in a porous layer. The cell used was 3 mm wide, 15 cm high and 1 m long and was sealed at the base. A lock region was set up at one end of the cell, bounded by two vertical lock gates which separated the source fluid from the main part of the Hele-Shaw cell and from its end. At the start of the experiment both lock gates were removed. The fluid was free to spread along the lower boundary and to drain freely from the open end of the cell (figure 3). The length and depth of this initial block of fluid was varied between experiments.

The working fluid was golden syrup of viscosity approximately 60 Pa s so that the current had typical Reynolds number 10^{-4} – 10^{-5}. During the experiment, we measured the lateral extent and shape of the current, and also the mass of fluid draining from the origin. The dipole moment Q was calculated at a series of times during the experiment by digitizing the shape of the current and calculating expression (2.3) using the trapezium rule. The results of this for a typical experiment are shown in figure 4. The dipole moment converges to a constant as the flow adjusts to the self-similar solution (figure 4) as predicted by the theoretical work of Kamin & Vazquez (1991). Figure 5 shows that the run-out distance of the current as measured in the experiments scales as $L \sim (Q\Omega)^{1/4}t^{1/4}$, as predicted by the similarity solution equation (2.6). In these two experiments, the initial aspect ratios of the fluid behind the lock gate h_0/L_0, were 1 and 2.7. Figure 6 illustrates the shape of the current in similarity space at four different times for the initial aspect ratio 1. This is in excellent accord with the analytical self-similar solution (2.6). Finally figure 7 shows the mass of fluid $M(t)$ which drains from the current at $x = 0$, and this is compared with the theoretical prediction, $M(t) \sim t^{-1/4}$.

In figures 4–7 the experimental observations are described well by the self-similar solution (2.6), confirming that this provides a very accurate description of the flow. The solution describes the experimental flow at intermediate times (Barenblatt 1996)

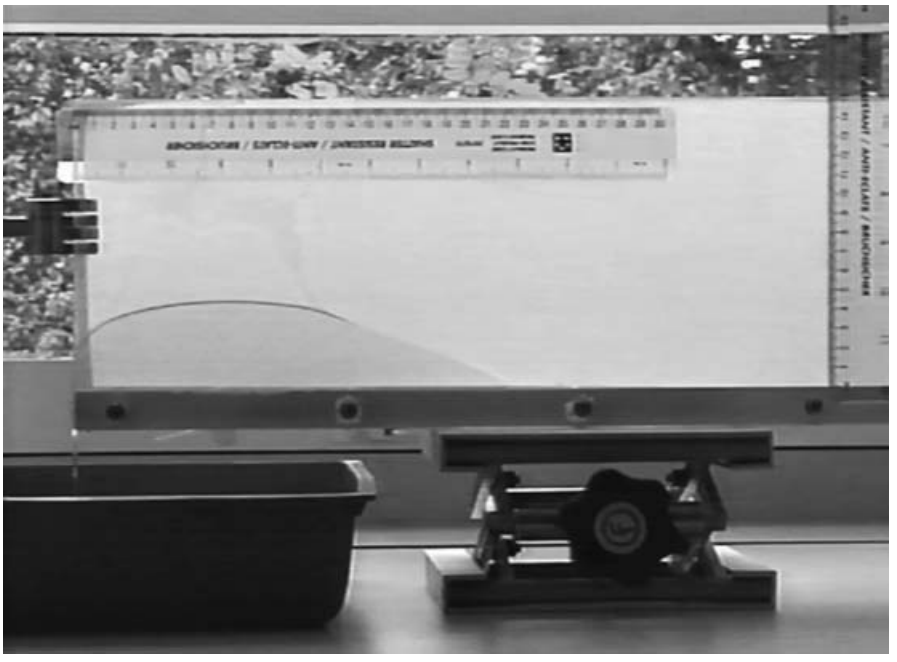

FIGURE 3. Photograph showing the experimental apparatus and the current slumping along the base of the Hele-Shaw cell.

once the fluid has evolved from the initial condition of the experiment to the self-similar solution, but before the current is strongly influenced by friction at the base of the cell. At such a late stage equation (2.1) no longer provides an accurate description of the flow.

3. Dipole gravity current which drains into a lower-permeability layer beneath

3.1. *Theory*

We now consider the effect of replacing the horizontal impermeable lower boundary in the flow discussed in § 2 with a thin horizontal layer of smaller permeability (see figure 8). This flow configuration may occur naturally if fluid were to invade a stratified rock. We focus on the case in which the layer of lower permeability has thickness b, which is small in relation to the depth of the current ($h \gg b$). Assuming that the pressure relative to hydrostatic falls to zero on the other side of the low-permeability layer, then the evolution equation takes the approximate form (Pritchard *et al.* 2001)

$$h_t = \Omega(hh_x)_x - \lambda h, \tag{3.1}$$

where $\lambda = \Omega K_b/Kb$, K_b the permeability of the lower layer and b its height.

In § 2 we saw that the dipole moment of the height of the free surface of the flow remained constant. Now the rate of change of the dipole moment with time is given by

$$\frac{\mathrm{d}}{\mathrm{d}t}\int_0^L xh\,\mathrm{d}x = L\dot{L}h(L,t) + [xhh_x]_0^L - \int_0^L \lambda xh\,\mathrm{d}x = -\lambda\int_0^L xh\,\mathrm{d}x. \tag{3.2}$$

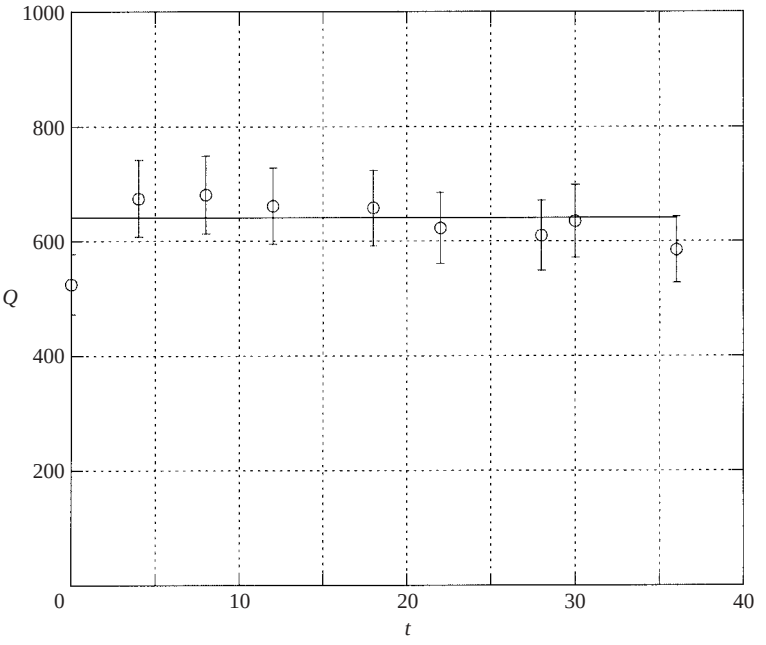

FIGURE 4. Plot of the evolution of the dipole moment of an experimental current with time, together with a straight line demonstrating the convergence of the dipole moment to a constant. The measurements of the dipole moment are shown with 10% error bars.

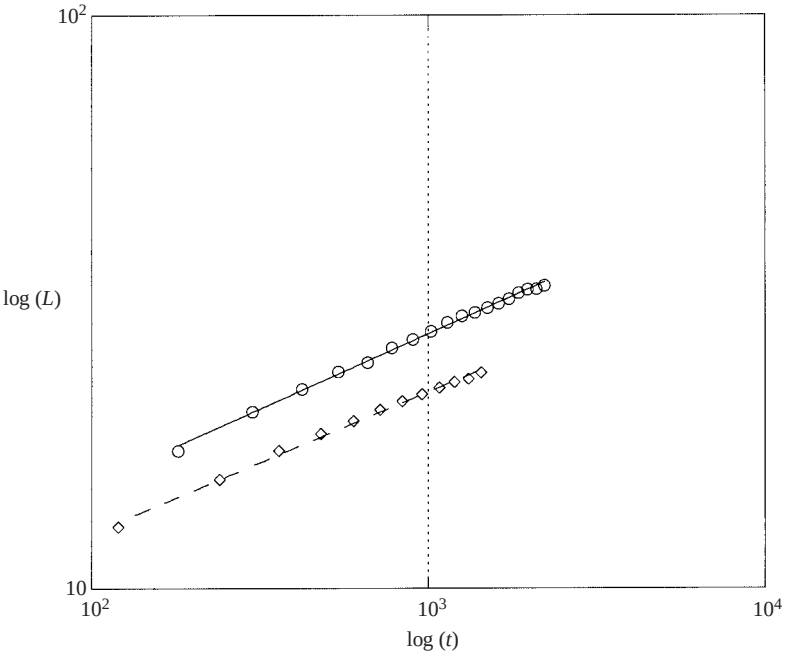

FIGURE 5. The log of the measured run-out distance of two currents ($\diamond$, $\circ$) against log of time. Best fit lines give exponents for time dependence of 0.26 and 0.25, compared with the theoretical value 0.25.

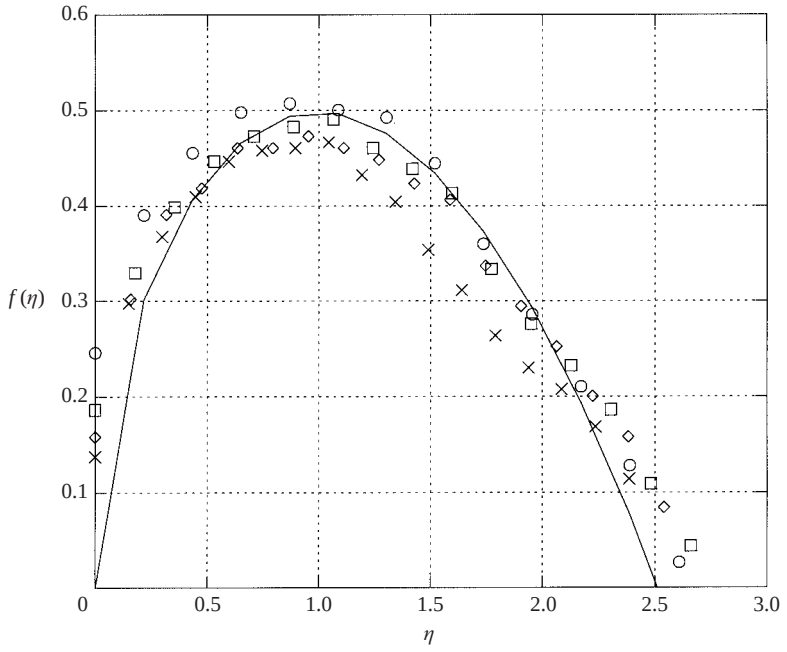

FIGURE 6. Measured shape of the current compared with the theoretical shape at times $t = 8, 18, 28, 36$ s ($\circ$, $\square$, $\diamond$, $\times$ respectively) for one of the experiments.

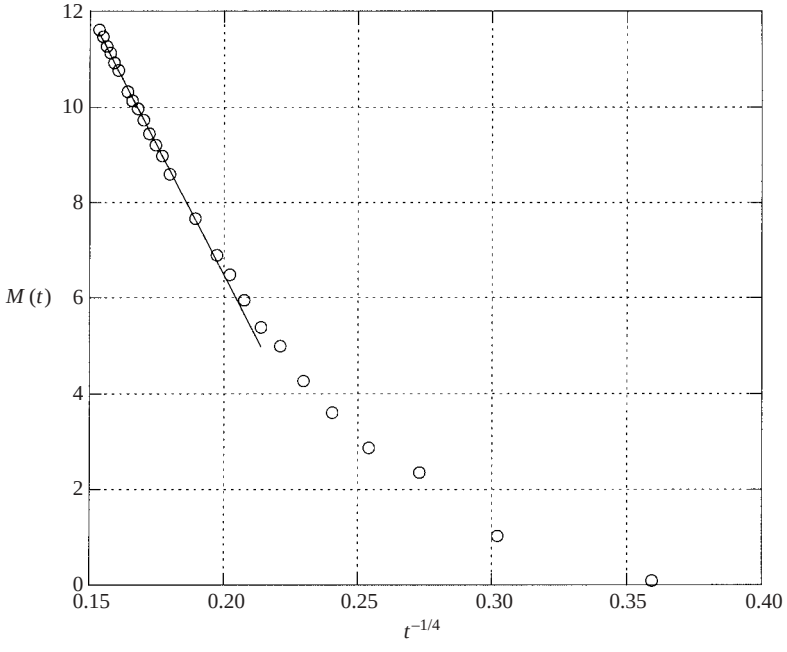

FIGURE 7. A typical plot of the mass of fluid $M(t)$ drained from the origin during an experiment ($\circ$) plotted against $t^{-1/4}$, so that time increases towards the origin.

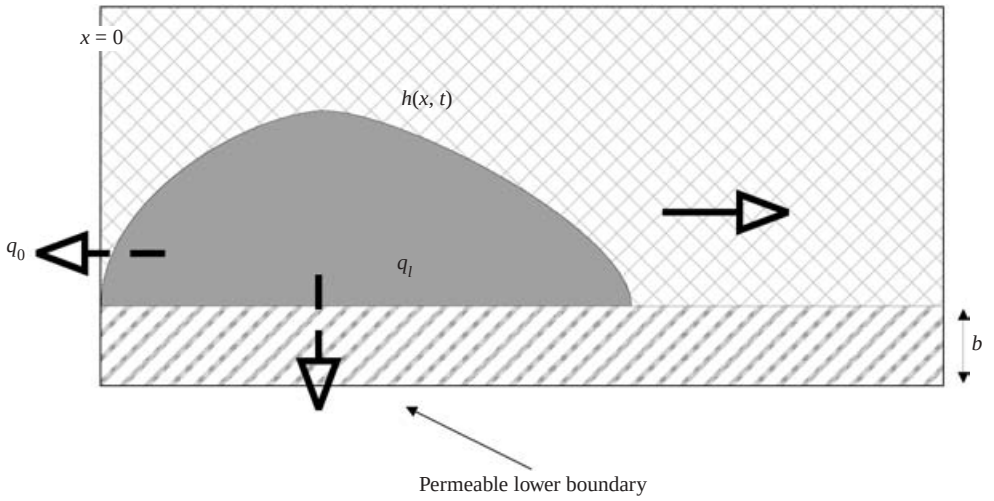

FIGURE 8. Diagram showing the spreading of a mound of fluid over a thin permeable layer with drainage into the layer and free draining at $x = 0$, with the volume fluxes through the lower layer q_l, and through the origin q_0, marked.

Equation (3.2) implies that the dipole moment decays exponentially with time. By using the transform

$$H = h\exp(\lambda t), \quad \tau = \frac{1-\exp(-\lambda t)}{\lambda}, \tag{3.3}$$

equation (3.1) may be re-expressed in the form

$$H_\tau = \Omega(HH_x)_x, \tag{3.4}$$

and so it may be seen that the motion of the current is described by a solution of the form presented in § 2, but now accounting for a slowly evolving dipole moment. This transform was first suggested by Gurtin & MacCamy (1977) in the context of the diffusion of biological populations. Transforming back to the original coordinates we now obtain the solution

$$h = \left(\frac{Q}{\Omega}\right)^{1/2}\left(\frac{1-\exp(\lambda t)}{\lambda}\right)^{-1/2} f(\eta)\exp(-\lambda t), \tag{3.5}$$

$$f(\eta) = \tfrac{1}{6}\left((40)^{3/8}\eta^{1/2} - \eta^2\right), \tag{3.6}$$

where the transformed similarity variable is defined by

$$\eta = \frac{x}{(Q\Omega)^{1/4}\left(\dfrac{1-\exp(-\lambda t)}{\lambda}\right)^{1/4}}. \tag{3.7}$$

This solution is valid for $h \gg b$, which in turn requires

$$b \ll Q^{1/3}, \quad t > \frac{1}{\lambda}\ln\left(\frac{b}{Q^{1/3}}\right). \tag{3.8}$$

Combining (3.5) and (3.7) it is seen that $Q = Q_0\exp(-\lambda t)$ as expected.

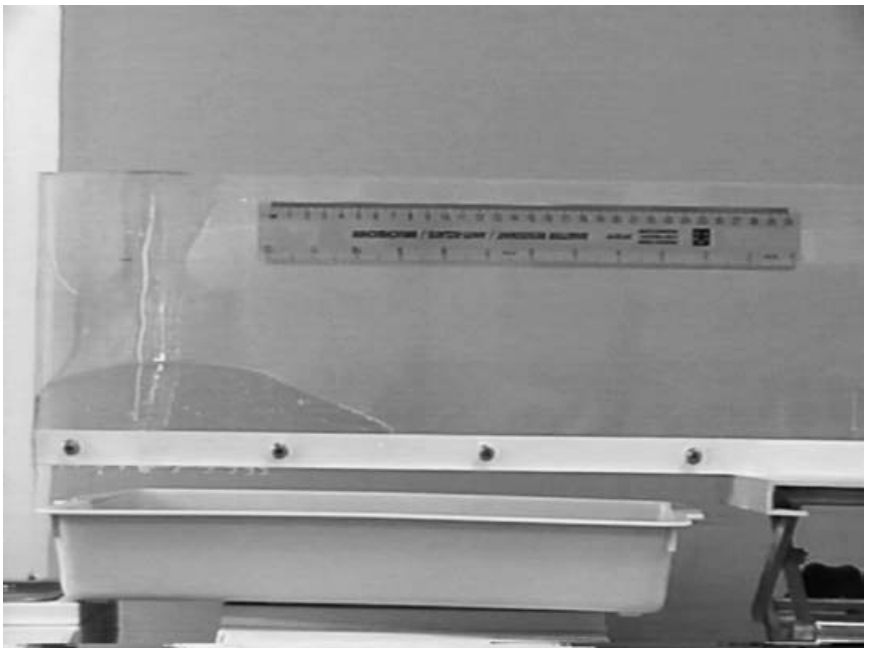

FIGURE 9. Photograph showing the experimental apparatus and the current slumping along the base of the Hele-Shaw cell whilst draining through a permeable lower boundary.

3.2. *Experiments*

We have conducted a series of experiments to compare with the theoretical work presented in § 3.1. The experimental apparatus involves the same Hele-Shaw cell as described in § 2.2 except that the width of the cell was increased to 4 mm, and the lower 2 cm of the cell was now held open with a gap of 1 mm. The cell was suspended above the laboratory bench by two jacks so that the fluid could drain out at the base (figure 9). This serves as a model of a layered permeable medium. As in § 2, the working fluid was golden syrup, and in each experiment fluid was released from a rectangular initial shape confined between two removable lock gates.

Figure 10 shows values of the dipole moment calculated from the current profiles taken at a series of times in a typical experiment. These measurements were carried out in the same way as those in § 2.2. The data demonstrate that the dipole moment decays exponentially as predicted by equation (3.2).

In figure 11 we illustrate the variation of the fourth power of the lateral extent of the current, L^4, as a function of $\exp(-\lambda t)$ as derived from the experimental measurement of L and t. The data collapse onto a straight line as predicted by the model until $\exp(-\lambda t) \approx 0.1$, which corresponds to a time $t = 100\,\mathrm{s}$. For longer times the experimental observations diverge from the theoretical model because the depth of the current has decreased towards the thickness of the low-permeability layer. Subsequently, the low-permeability layer is relatively deep compared to the current, the condition $h \gg b$ (§ 3.1) is violated, and the motion is no longer described by equation (3.1). This late stage of the flow may be described using the approach of Acton, Huppert & Worster (2001) and Pritchard & Hogg (2002). In figure 12 we compare the shape of the current at $t = 80\,\mathrm{s}$ with the theoretical prediction of equation (3.5), and obtain very good agreement.

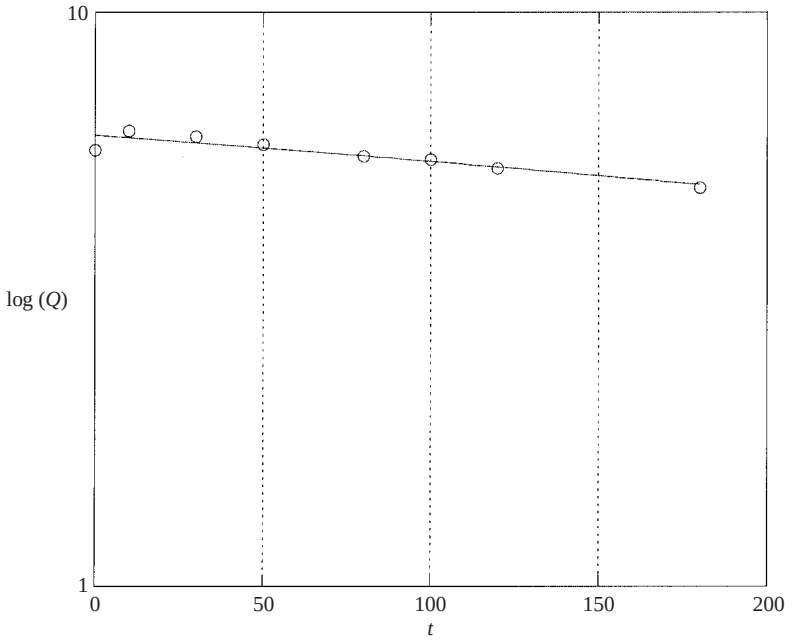

FIGURE 10. Plot of the evolution of the measured dipole moment of a draining experimental current with time, together with a straight line demonstrating that the dipole moment decays exponentially with time.

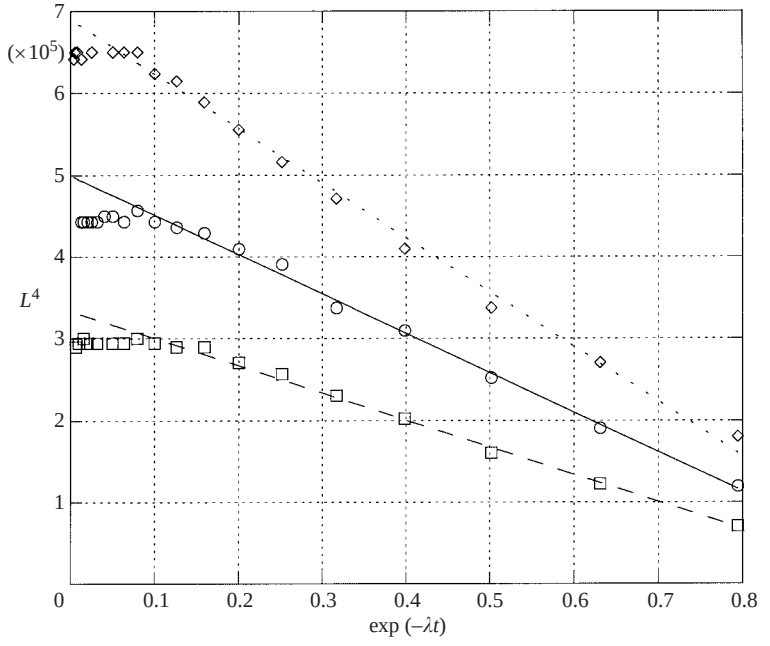

FIGURE 11. The measured run-out distance of three dipole experiments which drain through a lower layer (○, □, ◇). Plotted is L^4 against $\exp(-\lambda t)$; initially the data lie along a straight line so that L^4 varies linearly with $\exp(-\lambda t)$ as predicted. Time increases towards the origin in this plot.

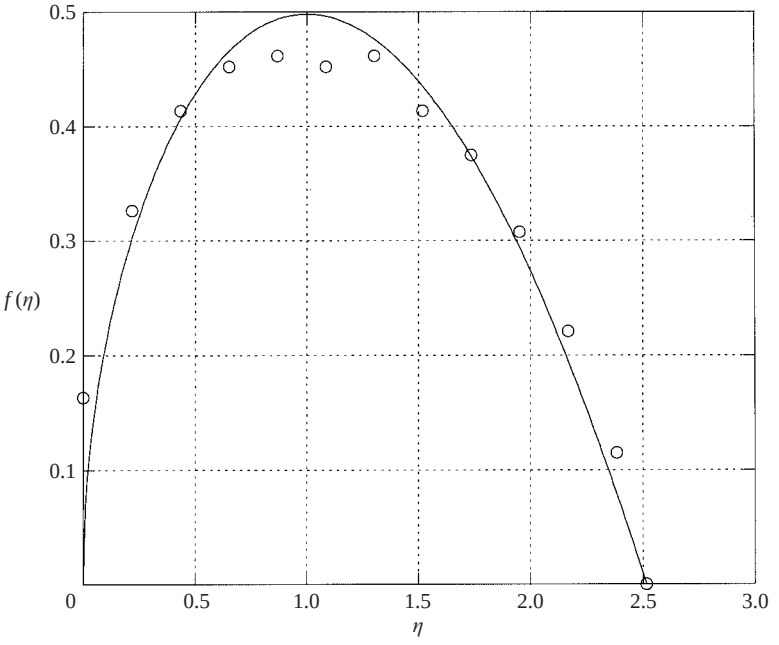

FIGURE 12. The typical shape of the current for one experiment at time $t = 80$ (○) which corresponds to $\exp(-\lambda t) = 0.16$. The theoretical shape function for the current is shown for comparison.

3.3. *Loss of fluid to the layer below and to the well*

The solutions presented in § 3.1 have implications for the dispersal of pollutants in an aquifer, or the injection of chemical treatments into an oil reservoir. In these situations it may be possible for fluid to drain into a lower-permeability layer in the rock and to drain back at the source. It is of considerable interest in these cases to have some knowledge of the fraction of injected fluid which remains in the porous layer. To that end we now examine the volume flux of fluid from the current. First, the flux into the source $q_0(t)$ is defined by

$$q_0(t) = h \left.\frac{\partial h}{\partial x}\right|_0 ; \tag{3.9}$$

secondly the flux into the underlying porous layer $q_l(t)$ as defined by

$$q_l(t) = \int_0^{L(t)} \lambda h \, \mathrm{d}x. \tag{3.10}$$

These two fluxes are shown in figure 8, and are given by the expressions

$$q_0 = -\frac{1}{72}(40)^{3/4} \left(\frac{Q^3}{\Omega}\right)^{1/4} \left(\frac{1-\exp(-\lambda t)}{\lambda}\right)^{-5/4} \exp(-2\lambda t), \tag{3.11}$$

$$q_l = -\frac{1}{18}(40)^{3/4} \left(\frac{Q^3}{\Omega}\right)^{1/4} \left(\frac{1-\exp(-\lambda t)}{\lambda}\right)^{-1/4} \lambda \exp(-\lambda t). \tag{3.12}$$

Comparison of these two equations shows that the drainage back to the source is

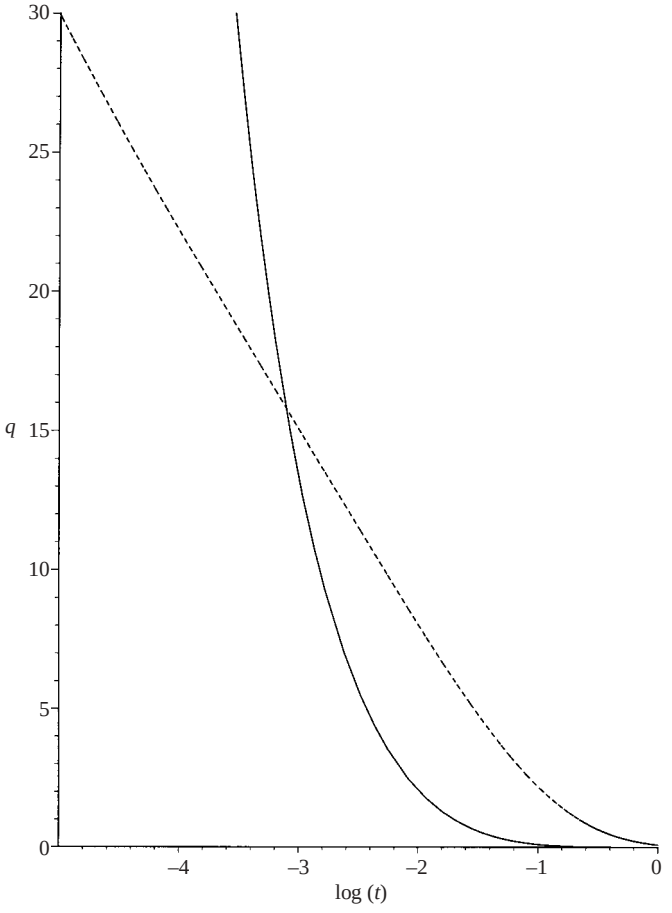

FIGURE 13. The evolution of the fluxes through the origin (solid) and through the lower layer (dotted) for the dipole solution which drains through a lower layer.

greater for short times $t < (1/\lambda)\ln(5/4)$, while the loss of fluid into the formation is dominant at long times. The variations of the fluxes with time are compared in figure 13.

Using the fluxes (3.11) and (3.12), we can calculate the volumes of fluid supplied by the current to both the underlying layer and the origin over times $t_0 < t < \infty$. If we assume that the solution (3.5) applies at time t_0 then we may consider the fractions of fluid supplied to the origin and the underlying layer as a parametric function of t_0 and hence of the initial aspect ratio (defined as the maximum height to length of the current).

Integration of equations (3.11), (3.12) from $t = t_0$ to ∞ yields the expressions for (i) V_0, the volume of fluid which drains back at the origin

$$V_0 = \frac{(40)^{3/4}}{72}\left(\frac{Q^3}{\Omega}\right)^{1/4}\lambda^{1/4}\left\{\frac{4}{\lambda}(1-\exp(-\lambda t_0))^{-1/4}\exp(-\lambda t_0) + \frac{16}{3\lambda^2} - \frac{16}{3\lambda^2}(1-\exp(-\lambda t_0))^{3/4}\right\}, \quad (3.13)$$

and (ii) V_l, the volume of fluid that leaks into the lower layer

$$V_l = \frac{(40)^{3/4}}{18}\left(\frac{Q^3}{\Omega}\right)^{1/4}\lambda^{1/4}\left(\tfrac{4}{3} - \tfrac{4}{3}(1-\exp(-\lambda t_0))^{3/4}\right). \tag{3.14}$$

The total volume in the current at time t_0, $V_t = \int_0^L h(x, t_0)\,\mathrm{d}x$, is given by integrating equation (3.5) and has value

$$V_t = \frac{(40)^{3/4}}{18}\left(\frac{Q^3}{\Omega}\right)^{1/4}\left(\frac{1-\exp(-\lambda t_0)}{\lambda}\right)^{-1/4}\exp(-\lambda t_0). \tag{3.15}$$

Combining equations (3.13)–(3.15) we can now find the fraction which leaks into the lower layer $\mathscr{F}_l = V_l/V_t$ and the fraction which drains back to the origin $\mathscr{F}_0 = V_0/V_t$. We expect $\mathscr{F}_l$ and $\mathscr{F}_0$ to be functions of the aspect ratio of the current, h/L, at time t_0 .

To find the aspect ratio of the current at a time t_0 we evaluate the maximum height and length of the current by use of the solution (3.5). At the initial time t_0 the maximum height of the current is given by the solution

$$h(t_0) = \left(\frac{Q}{\Omega}\right)^{1/2}\left(\frac{1-\exp(-\lambda t_0)}{\lambda}\right)^{-1/2} f_{\max}\exp(-\lambda t_0), \tag{3.16}$$

where $f_{\max}$ is the maximum value taken by the shape function f. Similarly the horizontal extent of the current can be found from the solution,

$$L(t_0) = (Q\Omega)^{1/4}\left(\frac{1-\exp(-\lambda t_0)}{\lambda}\right)^{1/4}\eta_{\mathrm{end}}, \tag{3.17}$$

where η_{end} is the value of η at the nose of the current at which $f = 0$ in similarity variables. This leads to an expression for the aspect ratio h/L:

$$\frac{h}{L}(t_0) = \left(\frac{Q^3}{\Omega}\right)^{1/4}\left(\frac{1-\exp(-\lambda t_0)}{\lambda}\right)^{-3/4}\exp(-\lambda t_0)\frac{f_{\max}}{\eta_{\mathrm{end}}}. \tag{3.18}$$

In figure 14 we plot $\mathscr{F}_l$ and $\mathscr{F}_0$ as a function of the aspect ratio of the flow. As the aspect ratio h/L decreases, more of the fluid drains into the formation. However, even with an aspect ratio of 0.1, 5% of fluid drains back at the source. This result implies that for effective dispersal of a finite mass of chemical in an aquifer or oil reservoir system, then the fluid should be supplied over a prolonged period to ensure that it has a small aspect ratio h/L before the source is cut off.

4. Generalization of the model

4.1. *Theory*

The solution approach for equation (2.1) also applies to the more general family of equations

$$h_t = \kappa(h^\alpha h_x)_x, \tag{4.1}$$

parameterized by α. This equation describes the flow of a fluid in a number of different situations. For example the equation with $\alpha = 3$, describes the flow of a viscous free-surface gravity current in a two-dimensional channel and this has

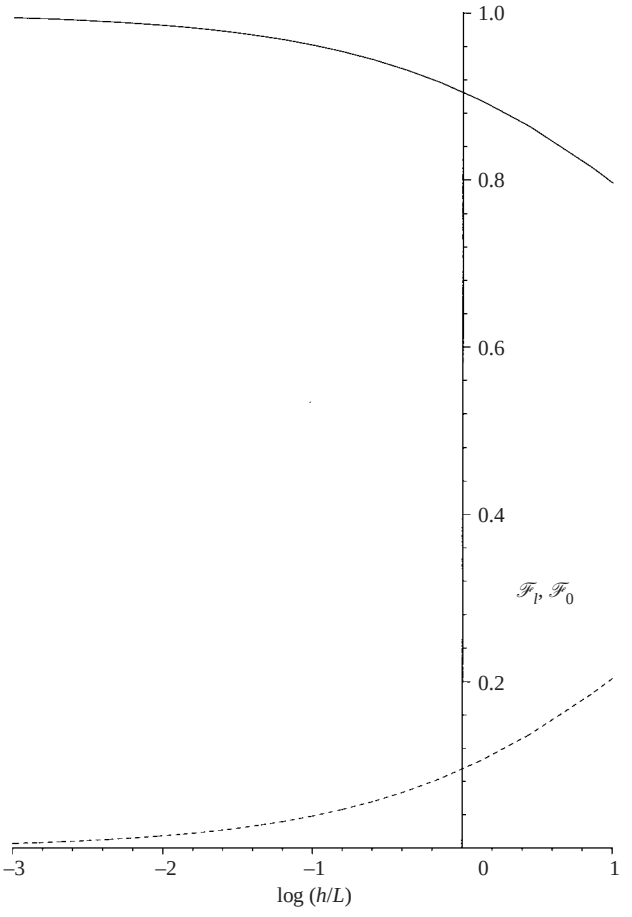

FIGURE 14. Plot showing the partitioning of the volume of the current to (i) drain back into the source region ($\mathscr{F}_0$ dotted) and (ii) drain into the formation ($\mathscr{F}_l$ solid). The figure illustrates the fractions as a function of the initial aspect ratio (h/L) of the current. $\lambda = 0.3$, $\Omega = 5$ and $Q = 5$.

been studied in detail (Smith 1969; Didden & Maxworthy 1982; Huppert 1982; Gratton & Minotti 1990; Diez, Gratton & Gratton 1992). More generally it describes the situation of a gravity current spreading through a porous medium in which the permeability varies as

$$k = k_0 y^{\alpha-1}, \tag{4.2}$$

where y is the vertical axis with origin at the base of the current (Huppert & Woods 1995). This is also equivalent to flow in a Hele-Shaw cell in which the narrow gap width varies vertically according to the relation

$$b = b_0 y^{\frac{\alpha-1}{2}}. \tag{4.3}$$

In the case $\lambda = 0$, which corresponds to the case of no loss through the lower boundary, the dipole moment

$$\int_0^L xh(x,t)\,\mathrm{d}x = Q, \tag{4.4}$$

is again conserved and so we can pose a solution to the equation of the form

$$h = At^{\beta} f\left(\frac{x}{Bt^{\gamma}}\right), \tag{4.5}$$

where $x/(Bt^{\gamma})$ is our similarity variable η. Substituting this into equation (4.1) we find that

$$\left.\begin{aligned} h(x,t) &= \kappa^{-\frac{1}{\alpha+1}} Q^{\frac{1}{\alpha+1}} t^{-\frac{1}{\alpha+1}} \left(C\eta^{\frac{\alpha}{\alpha+1}} - \frac{\alpha}{2(\alpha+1)}\eta^{\frac{2\alpha+2}{\alpha+1}}\right)^{1/\alpha}, \\ \eta(x,t) &= \frac{x}{\kappa^{\frac{1}{2(\alpha+1)}} Q^{\frac{\alpha}{2(\alpha+1)}} t^{\frac{1}{2(\alpha+1)}}}. \end{aligned}\right\} \tag{4.6}$$

On substitution of equation (4.6) into the integral condition (4.4) we obtain

$$\int_0^{\eta_e} \left(C\eta^{\frac{\alpha}{\alpha+1}} - \frac{\alpha}{2(\alpha+1)}\eta^{\frac{2\alpha+2}{\alpha+1}}\right)^{1/\alpha} \mathrm{d}\eta = 1, \tag{4.7}$$

where η_e is the end point of the current in similarity variables, and is given by

$$\eta_e = \left(\frac{2C(\alpha+1)}{\alpha}\right)^{\frac{\alpha+1}{\alpha+2}}. \tag{4.8}$$

C may be determined numerically from (4.7) and (4.8) for a given value of α. For example when $\alpha = 3$, we find $C = 0.7029$ to four decimal places.

The equation

$$h_t = \kappa(h^{\alpha} h_x)_x - \lambda h, \tag{4.9}$$

may be solved using a similar method to that in § (3.1); the transform

$$H = h\exp(\lambda t), \quad \tau = \frac{1-\exp(-\alpha\lambda t)}{\alpha\lambda}, \tag{4.10}$$

reduces equation (4.9) to an equation of the form of (4.1) and the above solutions may then be re-interpreted.

4.2. *Experiments*

To test the theoretical predictions (4.6) we have conducted some experiments in which a free-surface viscous flow spreads along a channel $x > 0$, whilst draining freely from the impermeable channel base at $x = 0$. This corresponds to the case $\alpha = 3$ in the above theory. We used a small Perspex flume tank of width 20 cm, height 25 cm and length 1 m. Initially the fluid is held between two adjustable lock gates at the open end of the flume tank; then both gates are removed so that fluid is free to drain out of the channel at the open end and spread along the base of the channel. Again we used golden syrup for these experiments. This is sufficiently viscous to ensure a Reynolds number $Re \leqslant 0.1$. In each experiment we measure the length of the current, the mass of fluid drained at $x = 0$ and the shape of the free surface. In figure 15 we show the variation of the run-out distance of the three experimental currents characterized by initial aspect ratios 0.9, 0.4 and 0.5. The aspect ratio is again defined by the ratio of the initial height to initial length of the fluid held behind the lock gates. All three sets of data are in good accord with the predictions of the theoretical solutions. The shape of the second of these currents is plotted in figure 16, compared with shape of the analytic solution. Finally in figure 17 the mass of fluid $M(t)$ drained at the origin is plotted for the third experiment. This agrees well with the theoretical prediction that $M(t) \sim t^{-1/8}$.

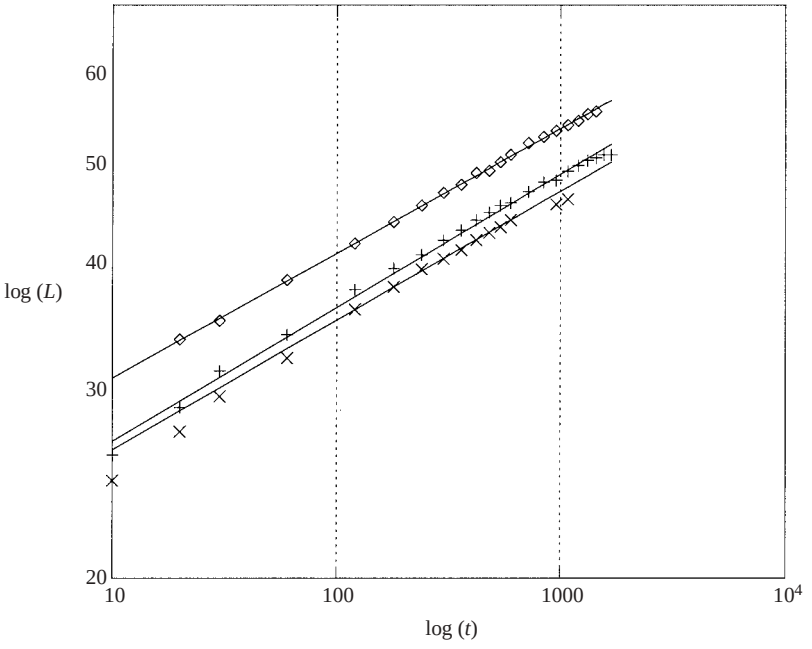

FIGURE 15. Plot showing the log of the run-out distance of three two-dimensional dipole experiments ($\diamond$, $+$, $\times$) against log of time; the exponents for the run-out are 0.122, 0.118, 0.127 compared with the theoretical value 0.125.

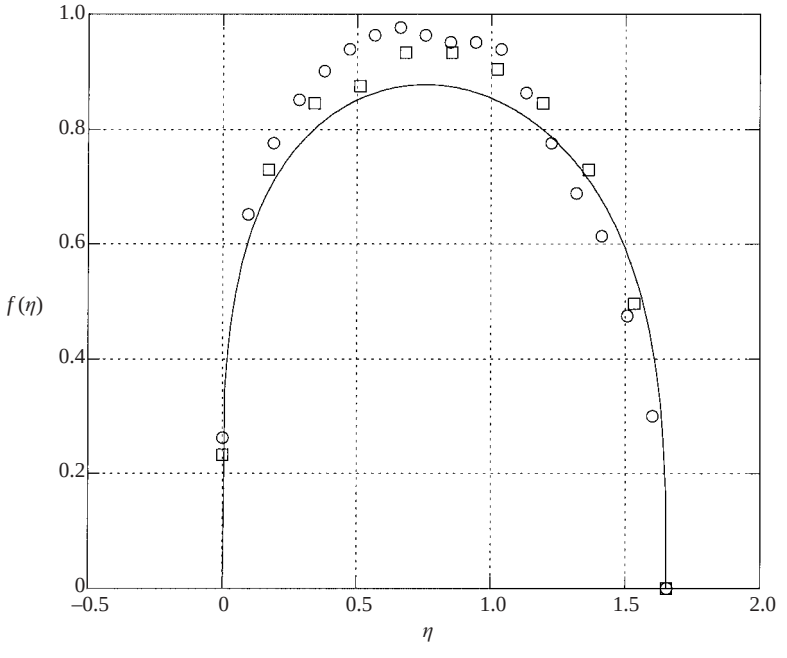

FIGURE 16. Measured shape of the current at times $t = 30, 420$ s ($\circ$, $\square$) during one experiment plotted with the theoretical shape function for comparison.

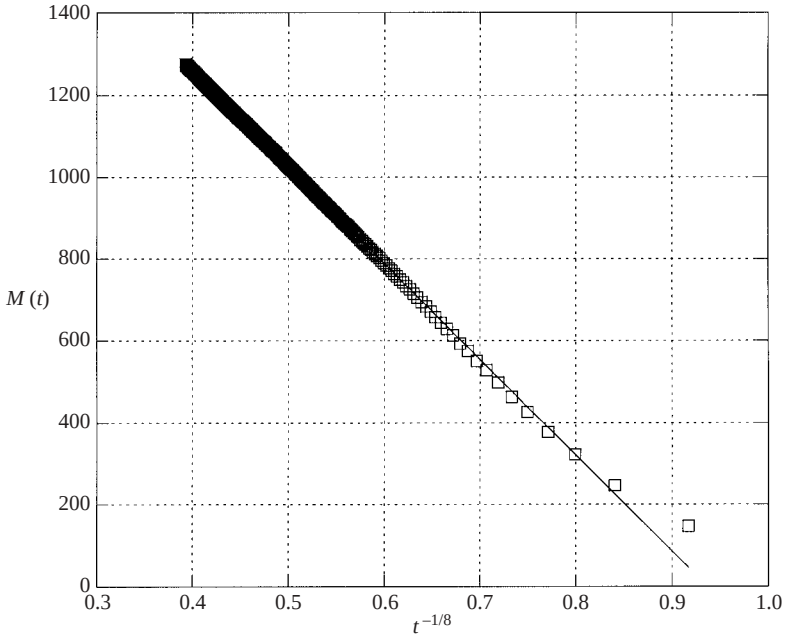

FIGURE 17. The mass of fluid $M(t)$ drained at the origin for one experiment (□) plotted against $t^{-1/8}$ along with a best fit line to demonstrate that the mass is a linear function of $t^{-1/8}$. Time increases towards the origin in this plot.

5. Summary

We have presented a series of models to describe the gravity-driven flow through a stratified porous layer, including the effects of drainage at the base of the layer and back to the origin. Analogue experiments conducted in a Hele-Shaw cell have confirmed that, for a flow which may drain freely at one end of the cell but with no draining through its base, then the dipole moment Q

$$Q = \int_0^{L(t)} xh(x,t)\,\mathrm{d}x, \tag{5.1}$$

of the flow is conserved, where Q is defined in terms of the height of the free surface $h(x,t)$ (Barenblatt & Zel'dovich 1957). In these experiments capillary forces were not found to be important; however the gravity–capillary force balance has been studied in detail by Bernis, Hulshof & King (2000), and similar experimental work to verify these solutions could be conducted.

We then showed that with draining through the base of the layer, as may arise in a stratified porous medium, the dipole moment decays exponentially. For such flows we found that initially the loss of fluid from the current is dominated by the drainage back into the source region $x = 0$, but at long times $t > t_c = (1/\lambda)\ln(5/4)$, the loss of fluid from the current is dominated by drainage into the underlying less permeable layer. Further experiments in a Hele-Shaw cell were conducted and verified the accuracy of this solution.

Finally we considered an extension of the modelling approach to describe a free-surface gravity current slumping over an impermeable surface, and again obtained very good agreement with experiments.

Appendix

Here we present an alternative derivation of the dipole solution presented in § 2, to show that the members of a family of solutions are consistent, each with integral moments as conserved quantities. From these, the solutions with either (i) first moment conserved or (ii) the volume conserved reduce the integral equation for the shape function to a simpler form amenable to analytic solution.

If we again consider a similarity solution

$$h = At^{\alpha} f\left(\frac{x}{Bt^{\beta}}\right), \tag{A 1}$$

to the governing equation (2.1), then we obtain the differential equation

$$\alpha f - \beta \eta f' = (ff')', \tag{A 2}$$

where the prime denotes differentiation by the similarity variable. We also obtain one constraint on α and β that

$$2\beta = \alpha + 1. \tag{A 3}$$

We can now make progress on equation (A 2), by multiplying by $\eta^{-\alpha/\beta-1}$, and integrating by parts twice to obtain

$$\eta^{-\alpha/\beta} f = \eta^{-\alpha/\beta-1} ff' + \frac{1}{2}\left(\frac{\alpha}{\beta}+1\right)\eta^{-\alpha/\beta-2} f^2 + \frac{1}{2}\left(\frac{\alpha}{\beta}+1\right)\left(\frac{\alpha}{\beta}+2\right)\int_0^{\eta} \xi^{-\alpha/\beta-3} f^2 \,\mathrm{d}\xi, \tag{A 4}$$

where we have used the boundary conditions

$$\eta^{-\alpha/\beta-1} ff' = 0 \quad \text{at} \quad \eta = 0, \tag{A 5}$$

$$\left(\frac{\alpha}{\beta}+1\right)\eta^{-\alpha/\beta-2} f^2 = 0 \quad \text{at} \quad \eta = 0. \tag{A 6}$$

Equation (A 4) describes the shape function of the solution for any choice of α and β that is consistent with the relation (A 3) above. However, two particular choices for α and β allow us to dispense with the integral term in equation (A 4) and find a solution for the shape function in closed form without the need for further boundary conditions. These are $\alpha/\beta = -1$, which corresponds to the volume conservative current, and $\alpha/\beta = -2$, which corresponds to the current with first dipole moment conserved.

REFERENCES

Acton, J., Huppert, H. & Worster, M. 2001 Two-dimensional viscous gravity currents flowing over a deep porous medium. *J. Fluid Mech.* **440**, 359–380.

Barenblatt, G. 1996 *Scaling, Self-similarity and Intermediate Asymptotics*. Cambridge University Press.

Barenblatt, G., Entov, V. & Ryzhik, V. 1990 *Flow of Fluid through Natural Rocks*. Kluwer.

Barenblatt, G. & Zel'dovich, Y. 1957 On dipole solutions in problems of non-stationary filtration of gas under polytropic regime. *Prik. Math. Mekh.* **21**, 718–720.

Bear, J. 1972 *Dynamics of Fluids in Porous Media*. Dover.

Bernis, F., Hulshof, J. & King, J. 2000 Dipoles and similarity solutions of the thin film equation in the half line. *Nonlinearity* **13**, 413–439.

Boussinesq, J. 1903 Recherches théoriques sur l'écoulement des nappes d'eau infiltres dans le sol et sur débit de sources. *C. R. H. Acad. Sci., J. Math. Pures Appl.* **10**, 6–78, 363–394.

Didden, N. & Maxworthy, T. 1982 The viscous spreading of plane and axisymmetric gravity currents. *J. Fluid Mech.* **121**, 27–42.

Diez, J., Gratton, R. & Gratton, J. 1992 Self-similar solution of the second kind for a convergent viscous gravity current. *Phys. Fluids* A **4**, 1148–1155.

Gratton, J. & Minotti, F. 1990 Self-similar viscous gravity currents: phase plane formalism. *J. Fluid Mech.* **210**, 155–182.

Gurtin, M. & MacCamy, R. 1977 On the diffusion of biological populations. *Math. Biosci.* **33**, 35–49.

Huppert, H. 1982 The propagation of two-dimensional and axisymmetric viscous gravity currents over a rigid horizontal surface. *J. Fluid Mech.* **121**, 43–58.

Huppert, H. & Woods, A. 1995 Gravity driven flows in porous media. *J. Fluid Mech.* **292**, 55–69.

Kamin, S. & Vazquez, J. 1991 Asymptotic behaviour of solutions of the porous medium equation with changing sign. *SIAM J. Math. Anal.* **22**, 34–45.

Pritchard, D. & Hogg, A. 2002 Draining viscous gravity currents in a vertical fracture. *J. Fluid Mech.* **459**, 207–216.

Pritchard, D., Woods, A. & Hogg, A. 2001 On the slow draining of a gravity current moving through a layered permeable medium. *J. Fluid Mech.* **444**, 23–47.

Smith, S. 1969 On initial value problems for the flow in a thin sheet of viscous fluid. *Z. Agnew. Math. Phys.* **20**, 556–560.

Turcotte, D. & Schubert, G. 1982 *Geodynamics. Applications of Continuum Physics to Geological Problems*. Wiley.